MultiCraft

International Journal of Engineering, Science and Technology
Vol. 4, No. 2, 2012, pp. 169-176

INTERNATIONAL JOURNAL OF ENGINEERING, SCIENCE AND TECHNOLOGY

www.ijest-ng.com
www.ajol.info/index.php/ijest
© 2012 MultiCraft Limited. All rights reserved

Weld metal characterization of 316L(N) austenitic stainless steel by electron beam welding process

Benjamin Joseph[1], D. Katherasan[1], P. Sathiya[1]* and C. V. Srinivasa Murthy[2]

[1]*Department of Production Engineering, National Institute of Technology, Tiruchirappalli – 620 015, Tamil Nadu, INDIA*
[2]*Defence Research & Development Laboratory, Hyderabad – 500 058, Andhra Pradesh, INDIA*
[*]*Corresponding Author: e-mail: psathiya@nitt.edu, Tel.:+9- 431- 2503510, Fax. +91- 43- 2500133*

Abstract

Electron beam welding (EBW) is a fusion joining process that produces a weld by impinging a beam of high energy electron to the weld joint. EBW has been used widely due to its advantages like narrow weld zone and heat affected zone, low distortion and contamination etc. The present work is focused on EBW of 316L(N) austenitic stainless steel varying the welding parameters such as beam power and welding speed. This study is carried out by analyzing the mechanical and metallurgical properties of the welded material. The mechanical properties have been evaluated using tensile, impact, hardness and bend test in accordance with the ASTM standards. The metallurgical characteristics are further investigated through optical microscopy. The mechanical properties of the weld material are better than the parent material. The variations of the mechanical properties were related with the variations in the cooling rate of the weld metal. The change in the cooling rate has influenced the grain size which has in turn influenced the mechanical properties. The metallurgical factors such as the presence of the ferrite and its percentage were also considered to substantiate the variation in the characteristics of the weld metal.

Keywords: electron beam welding, 316L (N), beam current, gun voltage.

DOI: http://dx.doi.org/10.4314/ijest.v4i2.13

1. Introduction

Due to an increasing demand for high-speed and low distortion welding, electron beam welding (EBW) has become useful in the fabrication of engineering parts with low-distortion joints, although its application to large assemblies is often restricted by the need to use a vacuum environment. An outstanding feature of EBW is its ability to make exceedingly narrow, deep holes. EBW is a high energy welding process which irradiates the work piece material it melts and fusion of the material occurs but the vaporization of the material is less. This results in a deep and narrow keyhole formation. The greatest advantage of this technique is to get welds with a very high aspect ratio. The welds are deep, narrow, defect-free and joining rates are also found to be very high. The characteristics of the fusion zone depend upon a large number of parameters like thermal properties of materials. The mechanical and metallurgical properties of the weld is highly influenced by beam characteristics, such as beam power, welding speed, focal point location, focal spot size, etc. The ferrite percentage has a significant effect on deciding the characteristics of the weld. The cooling rate can affect the ferrite percentage. The study has been carried out to investigate the variation of the properties with the change in cooling rate.

Eagar et al. (1989) has conducted study on Fe-Ni-Cr alloy, to find the variation in ferrite number. The solidification time and cooling rate significantly altered the ferrite number of different samples. The microstructures of the weld and fusion zone were affected by the composition of the base metal and welding parameters. David et al. (1990) conducted a study on low Cr-Ni ratio alloy to find influence of welding parameters on the microstructure by evaluating the weld microstructure and dendrite structures. Yilbas et al. (1998) conducted a study to investigate the mechanical and metallurgical properties of electron beam welded austenitic 321 stainless steel. Analysis of the first and second law of thermodynamics of the welding process was carried out. It was found that the heat-affected zone increased as the work piece thickness increased and micro cracks were present at the fusion

zone. Jankowski et al. (2004) conducted a study of microhardness which is influenced by the grain size. Tjong et al. (1995) investigated the characteristics of the 316L weld. AISI 316L stainless steel was welded by the electron beam (EB) and laser techniques. Microstructural characteristics, hardness profile, creep rupture properties and creep damage of the welds were investigated. Fully austenitic microstructure was obtained in the two welds. The solidification structure of the welds consisted of the cellular and equated dendrites. Dey et al. (2009) have made bead-on-plate welds on austenitic stainless steel plates using an electron beam welding machine. Experimental data were collected as per central composite design and regression analysis was conducted to establish input–output relationships of the process. An attempt was made to minimize the weldment area, after satisfying the condition of maximum bead penetration. And the optimization was done using genetic algorithm. Kohyama et al. (1994) conducted a study on microstructure of electron beam welded and TIG welded 316 stainless steel to study the variation in microstructure due to dual ion radiation. Byun et al. (2003) has investigated on the effects of irradiation, test temperature, and strain on the deformation microstructures of a 316LN stainless steel have been investigated using a disk-bend method and transmission electron microscopy. Deformation microstructure changed progressively from a dislocation network dominant to a large stacking fault/twin band dominant microstructure with increasing radiation dose and with decreasing test temperature. Also, an increased strain level enhanced the propensity of deformation twinning. Arivazhagan et al. (2011) carried out investigations to study the microstructure and mechanical properties of AISI 304 stainless steel and AISI 4140 low alloy steel joints by Gas Tungsten Arc Welding, Electron Beam Welding and Friction Welding. For each of the weldments, detailed analysis was conducted on the phase composition, microstructure characteristics and mechanical properties. From the literature survey, it is observed that the process parameters like gun voltage, beam current, and welding speed affect the weld quality (Stoenescu et al. 2007 ; Molak et al. 2009 ; Reddy and Rao 2009; Kumar et al. 2010 ; Hegeman et al. 2011). In the present study the electron beam welding of 316L(N) austenitic stainless steel was done and mechanical and metallurgical testing were carried out to understand the variation in the properties of the weld.

2. Experimental procedure

The welding was done using the 60kV, 8kW welder of Techmeta, France. The machine was incorporated to do small scale welding. The system has electron gun, vacuum chamber and work piece manipulator. The vacuum pressure was maintained at 10-4 bar. Auto focusing system enabled the work to get maximum power on the work piece. Different energy levels were obtained by varying the gun voltage and beam current. Some trails were done to fix the welding speed at which the full penetration can be obtained in single pass. 316L(N) austenitic stainless steel was used for the experiment. 316L (N) is designed to overcome the pitting corrosion, sensitization etc. The elemental composition is shown in Table 1. The material was cut into a dimension of 105 X 300mm with a thickness of 8mm. It was welded by keeping zero gap and the material preparation were done by removing 1 micron from the edge and surface. Butt weld joint was made between the plates. Table 2 gives the welding parameters that have been used for the welding.

Table 1 Chemical composition of 316L(N)

Element (wt%)	C	Ni	Cr	Mn	P	S	Si	Mo	N	Ti	Nb	Cu	Fe
316L(N)	0.024	10.07	16.89	1.51	0.026	0.0016	0.42	2.16	0.0597	0.02	0.02	0.35	Bal

Table 2 Welding parameters for each specimen

Specimen.No	Process Parameters			
	Gun voltage kV	Beam current mA	Travel speed m/min	Energy kW
1	60	50	0.5	3
2	60	60	1	3.6
3	60	70	1.5	4.2

1 2 3

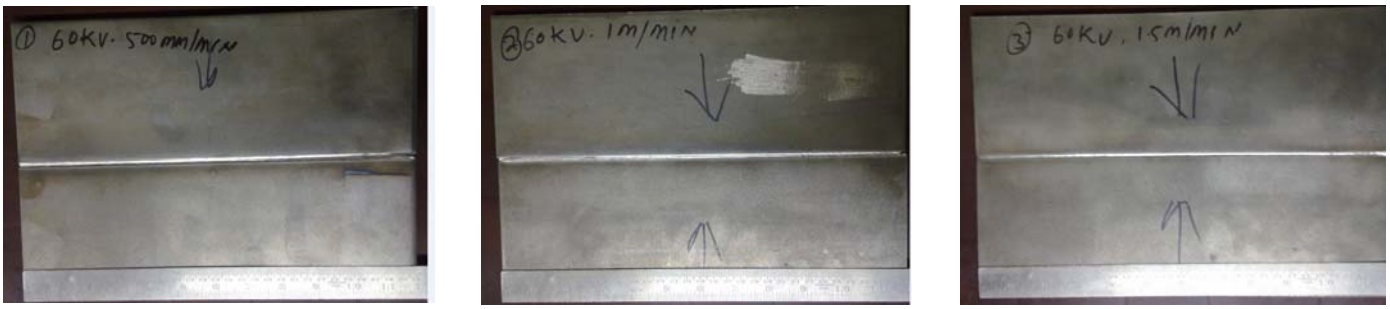

60kV,50mA,0.5m/min 60kV,60mA,1.0m/min 60kV,70mA,1.5m/min

Figure 1 Welded specimens

The Figure 1 shows the welded specimens. The specimens for testing were obtained from the welded plate and micro structural examinations were carried out at various cross sections of the weld. The specimens were mounted later flatted and then polished using SiC abrasive paper with grit ranges from 180 to 1200. Then the samples were lightly polished using 1µm alumina slurry. Samples were then washed, cleaned by acetone and then dried, followed by electrolytic etching in 10% oxalic acid at 9V for 30s (ASTM E3-11). Optical examination is performed using optical microscopy. Ferrite percentages were found using ferrite scope. The tensile testing is done on universal testing machine at room temperature (ASTM E8). Microhardness measurements were taken towards the longitudinal direction of the weld with a load of 1kgf for 20 seconds as per ASTM standards (ASTM E384-09). The face bend testing of the material was conducted to know the development of the cracks and fissures which will help to know the ductile nature of the weld material (ASTM E190-92). The specimens for Charpy test were taken as perpendicular to weld direction (ASTM E23). The Charpy impact test was conducted to get the toughness of the weld and it was conducted at -100 °C and -196 °C temperatures.

3. Results and discussion

3.1 Cooling Rate

Cooling Rate $\partial T/\partial t=-2\pi kV(T-T_0)^2/Q$ (Rosenthal, 1941) (1)

where k – Thermal conductivity in W/(m*K) ,T- Initial Temperature in K, To- Final temperature in K, V- welding speed and Q- energy input in W.

The cooling rate was calculated using Eq. (1) and the values are tabulated in Table 3.

Table 3 Cooling rate for each specimen

Sl No.	Q/V ratio	Cooling Rate(K/s)
1	6	356.9
2	3.6	594.89
3	2.8	764.86

3.2 Microhardness

Micro hardness values were measured and plotted in Figure 2 (ASTM E384-09). Figure 2 shows the variation of the hardness of the specimen at different zone like weld zone, heat affected zone (HAZ) and parent material. The hardness value of the HAZ is greater than the weld zone and parent material, because of the grains in the HAZ is finer than the weld zone and parent material. It shows that, as the energy input to welding speed ratio increases the hardness value of the weld zone is decreasing. The variation implies that as the ratio increases the grain size of the weld zone is increasing. Figure 3 shows the variation of hardness of weld zone against the ratio of energy input to the welding speed. The Q/V ratio and cooling rate is varying inversely. The lower cooling rate infers that the grains will get enough time to grow and form coarser grain and vice versa (Jankowski et al. 2004).

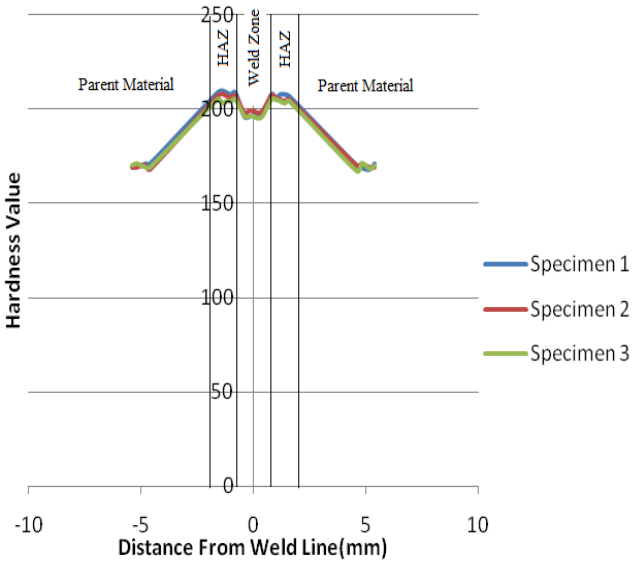

Figure 2 Hardness Value at different point from weld line

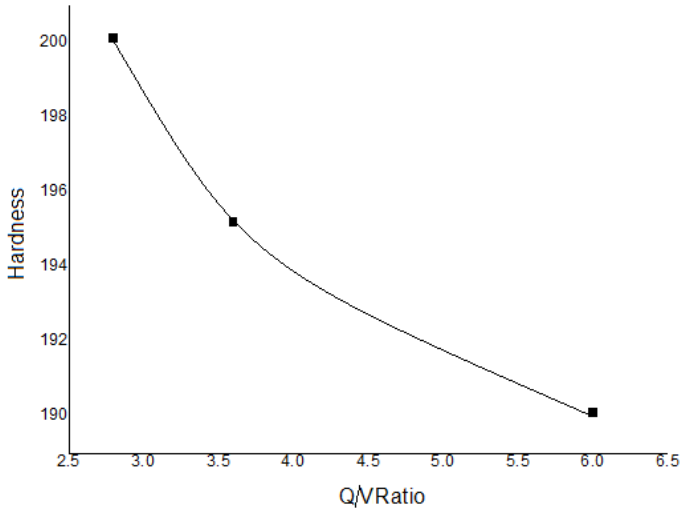

Figure 3 Microhardness Value as a function of Q/V Ratio

3.3 Transverse Tensile Test

The Figure 4 shows the schematic of the specimen used for tensile test (ASTM E8). The transverse tensile test results are tabulated in Table 4. The tensile tests were satisfactory since the specimen has been failed in the parent material. In nearly all cases the weld material is harder and showing better properties than the parent material. The cooling rate had significant effect on the tensile property of the weld. The failure in the parent material infers that the grain size is finer at the fused region (Hegeman et al. 2011).

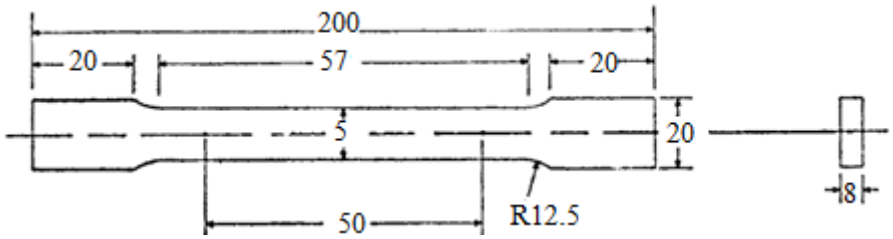

Figure 4 Schematic of specimen for tensile test (ASTM E8)

Table 4 Transverse tensile test results

Specimen No.	1	2	3
Ultimate tensile strength (MPa)	593.15	601.29	591.52
Base Material Strength (MPa)	560		

3.4 Face Bend Test

The Figure 5 shows the schematic of the specimen used for bend test (ASTM E190-92). From the face bend test results, the specimens did not fail even for bending at 180º at a bend radius of 16mm. The bend specimen microstructure was observed through the optical microscope, and no crack or fissures were observed in the weld.

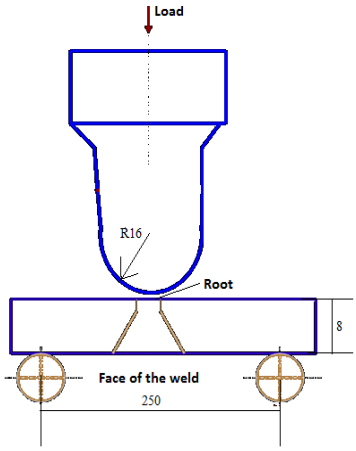

Figure 5 Schematic of face bend test

3.5 Ferrite Percentage

Table 5 gives the ferrite percentage obtained by using ferrite scope as tabulated. Figure 6 shows the variation of the ferrite percentage with Q/V ratio. Since no hot cracking was found on the weld it was clear the ferrite percent will be less than 8. When the ratio of the heat input to the welding speed increases the cooling rate decreases, it justified by the equation 1. When the cooling rate is high, the transformation time for the formation of the ferrite will be very low, this shows the lower Q/V ratio the ferrite percentage will be less (Eagar et al. 1989).

Table 5 Ferrite percentage

Sl.No	Ferrite percentage						Average
1	4.6	4.7	4.9	4.3	4.4	4.6	**4.6**
2	3.3	3.2	3.6	3.4	3.1	3.7	**3.4**
3	2.8	3.0	2.6	3.1	2.7	2.3	**2.8**

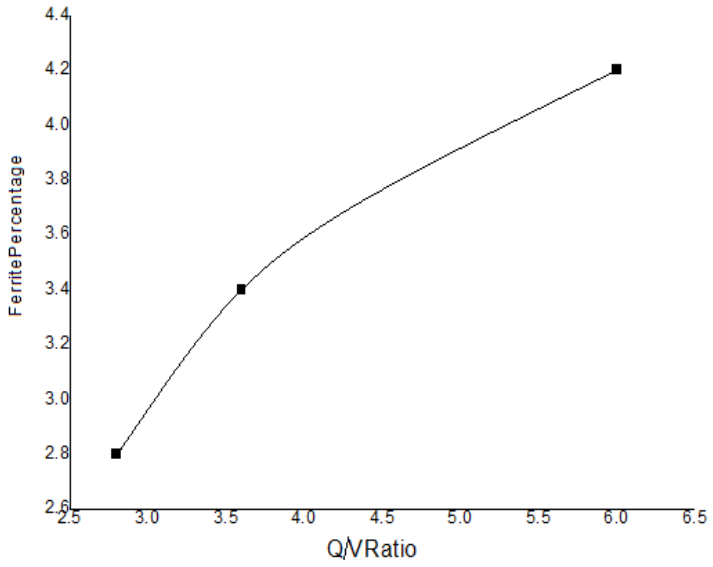

Figure 6 Ferrite percentages Vs. Q / V ratio

3.6 Impact Test

The Figure 7 shows the schematic of the specimen used for impact test (ASTM E23). The results of Charpy V- impact test are plotted in Figure 8. It shows that when Q/V ratio increases the energy absorbed by the material is reducing. The increase in the energy absorption implies that the ferrite content of the weld metal is variable. When the temperature is reduced the toughness of the material is reduced. The comparison of variation impact test results and the hardness test shows that both the values are

inversely proportional to the Q/V ratio. The base material has a toughness value of about 100J at -196^{0}C and around 133J at -100^{0}C.

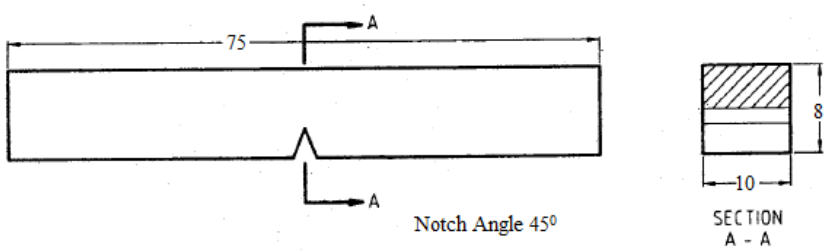

Figure 7 Schematic of the specimen prepared for the Charpy V Impact test (ASTM E23)

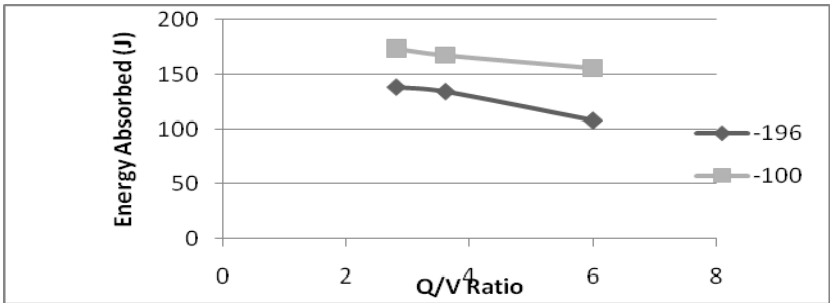

Figure 8 Impact test results Vs. Q / V ratio

3.7 Microstructure

The microstructure of the weld zone, parent material and fusion zone of the specimens are shown in Figures 9-11. Microstructure evaluation shows austenite matrix and dendrite ferrite. The dark lines seen in the microstructure are the grain boundaries. The spots seen are the inclusions and the carbides. As the energy input increases, the cooling time taken will be high, and in the microstructure it is nearly visible that there is variation in the grain size which is due to the variation in the grain growth time. By a rough evaluation of the area it is clear that the secondary phase formation has been varying according to change in the cooling rate which is related to the Q/V ratio. When the energy increases the grain size also increases. The energy input is increased the amount of secondary phase also varies (increase). When the cooling rate is increased the formation of secondary phase was decreased. The dendritic structures were visible in the microstructure and it is observed that the fusion zone has epitaxial grain growth.

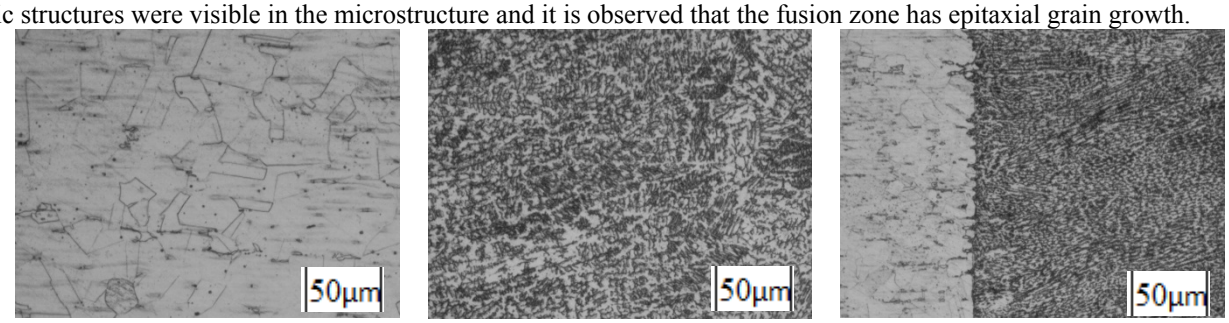

a) Base Material b)Weld Zone c)Fusion Line

Figure 9 Microstructure of Specimen 1

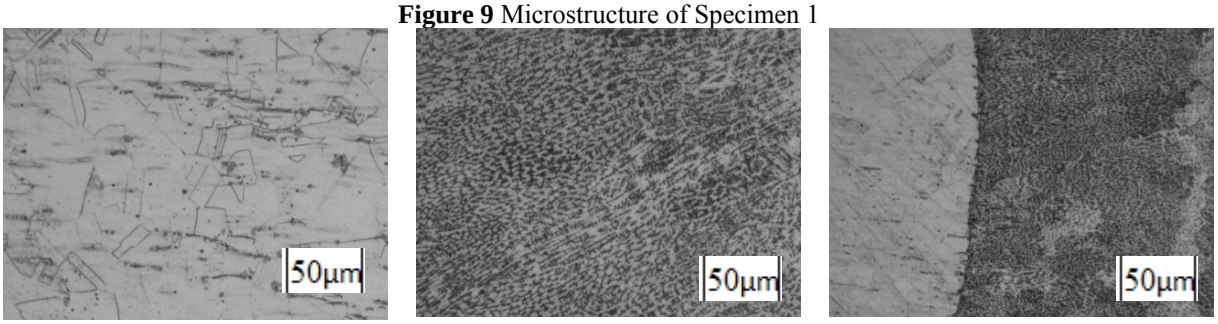

a) Base Material b)Weld Zone c)Fusion Line

Figure 10 Microstructure of Specimen 2

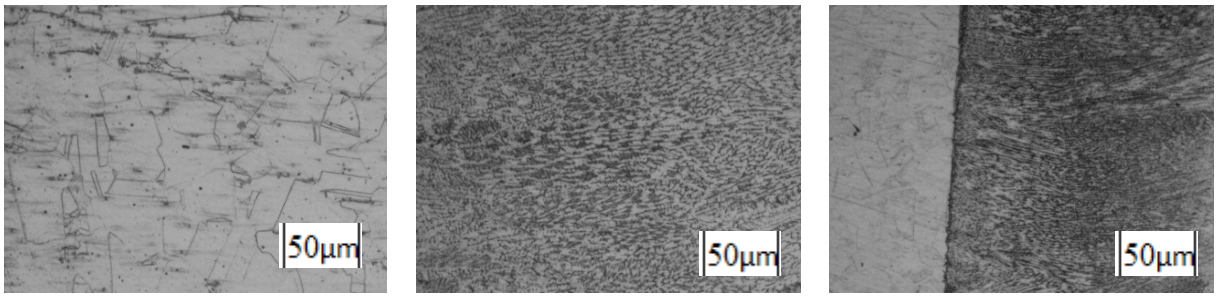

a) Base Material b)Weld Zone c)Fusion Line

Figure 11 Microstructure of Specimen 3

4. Conclusion

The characteristics of weld metal of 316L (N) welded by electron beam welding have been investigated at different beam power varying from 3kW to 4.2 kW. It is evident that the hardness of the material decreases with increases in Q/V ratio. This is due to variation the cooling rate. The toughness of the material decreased when Q/V ratio is increased, which is due to the variation in the grain size which is influenced by cooling rate. The toughness of the material gets reduced with the reduction in temperature. The face bend results showed that weld material is ductile and high energy welding process does not affect the ductility of the material. The tensile test shows welds were better than the parent material. The ferrite percentage is influenced by the cooling rate. The formation of ferrite depends on the phase transformation time and it has been evidently seen on the results. The microstructure shows the presence of the dendrite ferrite content in the weld metal. It is observed that the fusion zone has epitaxial grain growth.

Acknowledgement

We would like to express our gratitude to Mr. Dasharath Ram Yadav for offering us the distinguished opportunity to use the Electron beam welding trails at the Defence Research & Development Laboratory, Hyderabad – 500 058, Andhra Pradesh, India.

References

Arivazhagan, N., Surendra Singh, Satya Prakash, and Reddy, G.M., 2011. Investigation on AISI 304 austenitic stainless steel to AISI 4140 low alloy steel dissimilar joints by gas tungsten arc, electron beam and friction welding. *Materials and Design*, Vol. 32, pp. 3036–3050.

ASTM standard guide for preparation of metallographic specimens, E3-11.

ASTM standard test methods for tension testing of metallic materials, E8.

ASTM standard test methods for microindentation hardness of materials, E384-09.

ASTM standard test method for guided bend test for ductility of welds, E190-92(2008).

ASTM standard test methods for notched bar impact testing of metallic materials, E23.

Byun, T.S., Lee, E.H. and Hunn, J.D., 2003. Plastic deformation in 316LN stainless steel characterization of deformation microstructures. *Journal of Nuclear Materials*, Vol. 321, pp. 29–39

David, S.A., Vitek, J.M., Rappaz, M. and Boatner, L.A., 1990. Microstructure of Stainless Steel Single-Crystal Electron Beam Welds. *Metallurgical Transactions*, Vol. 21A, pp. 1753-1766.

Eagar, T.W., Allen, S.M. and Elmer, J.W., 1989. The influence of cooling rate on the ferrite content of stainless steel alloy. *International conference on recent trends in Welding Science and Technology*, *TWR*.

Ganesh Kumar, J., Chowdary, M., Ganesan, V., Paretkar, R.K., Bhanu Sankara Rao, K. and Mathew, M.D., 2010, High temperature design curves for high nitrogen grades of 316LN stainless steel. *Nuclear Engineering and Design*, Vol. 240, pp. 1363–1370.

Hegeman, J.B.J., Luzginova, N.V., Jong, M., Groeneveld, H.D., Borsboom, A., Stuivinga, M.E.C. and Van der Laan, J.G., 2011. Tensile properties of explosively formed 316L(N)-IG stainless steel with and without an electron beam weld. *Journal of Nuclear Materials*,Vol. 417, pp. 870–873.

Jankowski, A.F., Hayes, J.P., Saw, C.K., Vallier, R.F., Jackson Go and Ann Bliss, R., 2004. Grain Size Effect on the Micro-Hardness of BCC Metal Vapor Deposits. *TMS Letters, Materials Science and Technology*, Vol. 1, No. 8, pp. 175-176.

Kohyama, A., Kohno, Y. and Hishinuma, A., 1994. Microstructural evolution under dual ion irradiation and in-reactor creep of type 316 stainless steel welded joint. *Journal of Nuclear Materials*, Vol. 212-215, pp. 1579-1584.

Madhusudan Reddy, G. and Srinivasa Rao, K., 2009. Microstructure and mechanical properties of similar and dissimilar stainless steel electron beam and friction welds. *International Journal of Advanced Manufacturing Technology*, Vol. 45, pp. 875–888.

Molak, R.M., Krystian Paradowski, Tomasz Brynk, Lukasz Ciupinski, Zbigniew Pakiela and Krzysztof J. Kurzydlowski, 2009. Measurement of mechanical properties in a 316L stainless steel welded joint. *International Journal of Pressure Vessels and Piping*, Vol. 86, pp. 43–47.

Rosenthal, D., 1941. Mathematical theory of heat distribution during cutting and welding. *Welding Journal*, Vol. 20, No. 5, pp. 220–234.

Stoenescu, R., Schaublin, R., Gavillet, D. and Baluc, N., 2007. Welding-induced mechanical properties in austenitic stainless steels before and after neutron irradiation. *Journal of Nuclear Materials*, Vol. 360, pp. 255–264.

Tjong, S.C., Zhu, S.M., Ho, N.J. and Ku, J.S., 1995. Microstructural characteristics and creep rupture behaviour of electron beam and laser welded AISI 316L stainless steel. *Journal of Nuclear Materials*, Vol. 227, pp. 24-31.

Vidyut Dey, Dilip Kumar Pratihar, Datta, G.L., Jha, M.N., Saha, T.K. and Bapa, A.V., 2009. Optimization of bead geometry in electron beam welding using a Genetic Algorithm. *Journal of Materials Processing Technology*, Vol. 209, pp. 1151–1157.

Yilbas, B.S., Sami, M., Nickel, J., Coban, A. and Said, S.A.M., 1998. Introduction into the electron beam welding of austenitic 321-type stainless steel. *Journal of Materials Processing Technology*, Vol. 82, pp. 13–20.

Biographical notes

Dr. P.Sathiya is currently working as Associate Professor in Department of Production Engineering, National Institute of Technology, Tiruchirappalli, Tamilnadu, India. He did his Ph.D. (Welding) from National Institute of Technology, Tiruchirappalli, Tamilnadu, India. He has published forty five research papers in national and international journals and forty papers in conferences. His research interests are in broad areas of production engineering with specific interest in metal joining process, welding parameter optimization, fatigue and fracture.

Mr. D.Katherasan is currently perusing full time research scholar in Department of Production Engineering, National Institute of Technology, Tiruchirappalli, Tamilnadu, India. He has published three research papers in national and international journals and conferences. His research interests are in Optimization Techniques, and welding.

Mr. Benjamin Joseph is currently doing his post graduate in Manufacturing Technology, Department of Production Engineering, National Institute of Technology, Tiruchirappalli, Tamil Nadu, India. His fields of interests are in metal joining process and welding simulation.

Dr. C. V. Srinivasa Murthy is currently working as Scientist "G" in Defence Research & Development Laboratory, Hyderabad – 500 058, Andhra Pradesh, India.

Received May 2012
Accepted August 2012
Final acceptance in revised form September 2012